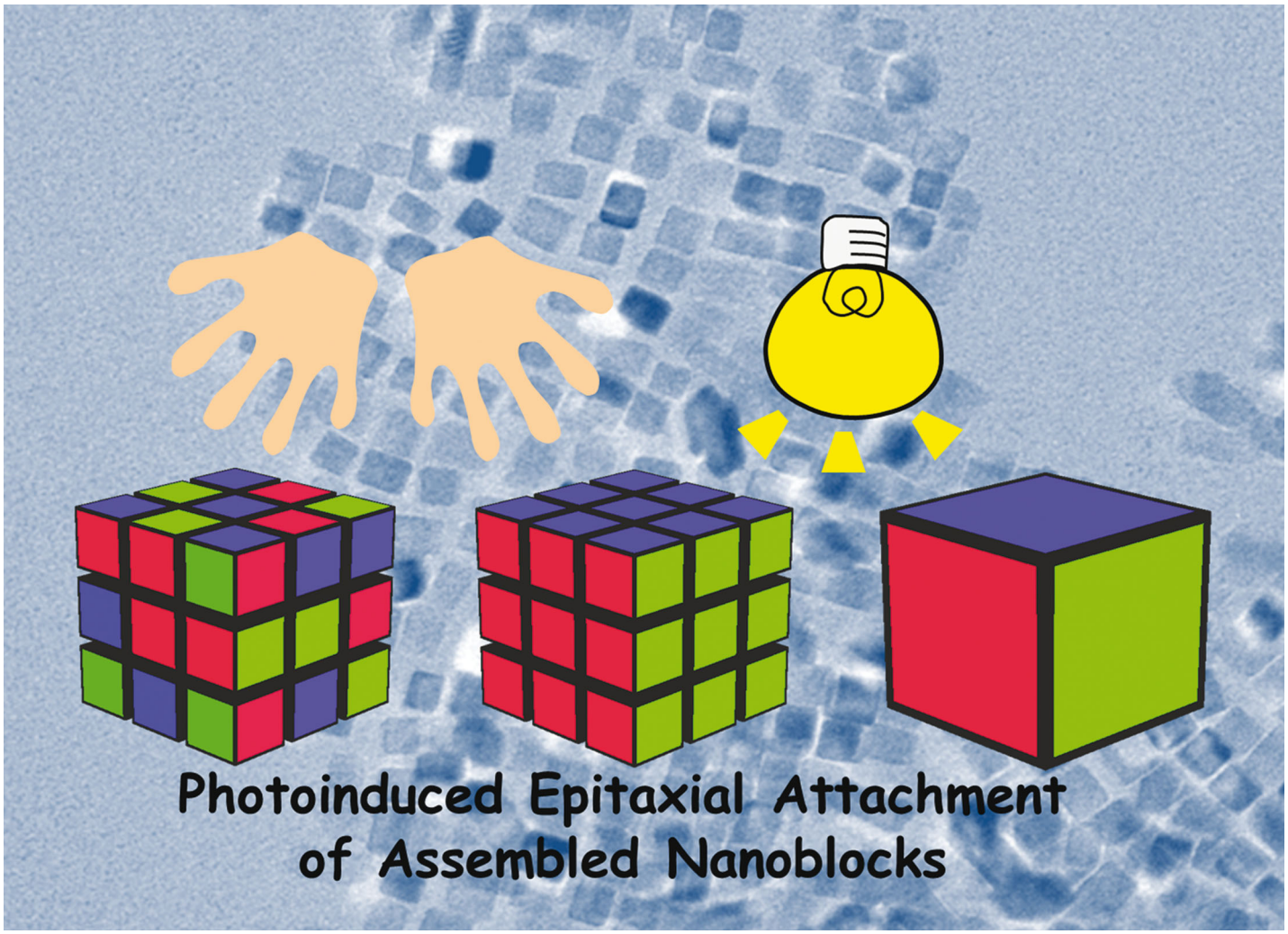

Showcasing research from the laboratory of Dr Hiroaki Imai, Department of Applied Chemistry, Faculty of Science and Technology, Keio University, Yokohama, Japan

UV-induced epitaxial attachment of TiO_2 nanocrystals in molecularly mediated 1D and 2D alignments

Anatase TiO_2 nanocrystals are crystallographically connected through UV-induced epitaxial attachments in ordered arrays.

As featured in:

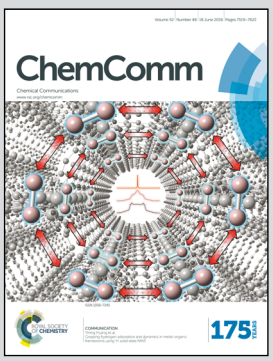

See Hiroaki Imai *et al.*, *Chem. Commun.*, 2016, **52**, 7545.

ROYAL SOCIETY OF CHEMISTRY

www.rsc.org/chemcomm

Registered charity number: 207890

ChemComm

COMMUNICATION

View Article Online
View Journal | View Issue

Cite this: *Chem. Commun.*, 2016, 52, 7545

Received 7th March 2016,
Accepted 21st April 2016

DOI: 10.1039/c6cc02001a

www.rsc.org/chemcomm

UV-induced epitaxial attachment of TiO_2 nanocrystals in molecularly mediated 1D and 2D alignments

Tomoyuki Hiraide, Hiroyuki Kageyama, Yoshitaka Nakagawa, Yuya Oaki and Hiroaki Imai*

Anatase TiO_2 nanocrystals were crystallographically connected through UV-induced epitaxial attachments in 1D and 2D arrays with photocatalytic decomposition of the organic mediator.

The bottom-up approach is an important route to nanometric materials that have great advantages over the bulky structures obtained using top-down processes.[1,2] Oriented attachment is a prospective non-classical bottom-up process for constructing a large-scale assembly of nanocrystals, such as biominerals.[2,3] One-, two-, and three-dimensional (1D, 2D, and 3D) crystals were found to be grown through the oriented attachment of nanoscale building blocks.[4]

Generally, superlattice structures are formed through the self-assembly of mono, binary, and ternary compounds of spherical nanocrystals.[5] Especially, the crystallographic orientation of superlattices is ordered by cubic-shaped nanocrystals.[6] Anisotropic shaped nanocrystals have the potential to form a molecular-mediated structure with a specific alignment.[7] 1D, 2D, and 3D microarrays of rectangular Mn_3O_4 nanoblocks were produced with controllable *a* and *c* axis orientations.[7c] In our previous report, 1D chains that consisted of crystallographically continuous Mn_3O_4 nanocuboids were achieved *via* the removal of organic mediators by plasma treatment and heat treatment.[8] Thus, such anisotropic nanoblocks have great potential in the construction of designed crystal morphologies.

Today, TiO_2 is used for various applications, such as photocatalysts, solar cell electrodes, and anodes of lithium-ion batteries.[4a,9–11] The shape and crystal surfaces of anatase TiO_2 nanocrystals were found to influence their photocatalytic activity.[10] Bulk heterojunction solar cells were fabricated with TiO_2 nanorods, polymers, and dyes.[11] Recently, the shape and crystal surfaces of TiO_2 nanoparticles have been finely controlled using organic molecules, such as oleic acid and oleylamine.[12] Moreover, the horizontal and vertical 2D superlattices were produced with anisotropic TiO_2 nanocrystals.[13] However, the selective assembly of 1D and 2D arrays has not yet been achieved using nanocrystals. The purpose of our present study is to examine selective 1D and 2D alignments of TiO_2 nanocrystals and their epitaxial attachments under UV irradiation. Single-crystalline TiO_2 alignments would be obtained through crystallographic fusion *via* the removal of organic molecules using a non-thermal process.

Dispersion of TiO_2 nanocrystals was induced using a solvothermal method based on previous studies.[12a,13] Five mmol of titanium butoxide (TB), 10 mmol of oleic acid (OA), and 15 mmol of oleylamine (OM) were mixed and stirred in 2.7 cm^3 of dehydrated ethanol. The mixture, in a Teflon vessel, was put into a larger Teflon vessel, and a 10 cm^3 mixture of dehydrated ethanol and pure water (ethanol/water = 24 in volume) was poured around the smaller vessel. The solvothermal process was carried out at 180 °C for ~18 h in a stainless steel autoclave. The precipitate at the bottom of the dispersion was extracted, and then toluene, OA, and OM were added. The precipitate obtained by the centrifugation of the toluene dispersion was redispersed in hexane. A transmission electron microscope (TEM, FEI Tecnai G2 F20) operated at 120–200 kV was used to observe the nanostructures of the products. The organic compounds in the obtained powders were analyzed using the KBr method using Fourier transform infrared spectroscopy (FTIR, Jasco FT/IR-4200). UV light from a super high-pressure UV lamp (Ushio UPM2-252Q) through visible and near infrared filters was irradiated onto the nanocrystals for the decomposition of the organic molecules.

Anatase TiO_2 nanocrystals were obtained as a dispersion in toluene. The crystalline phase was confirmed by lattice fringes observed using high-resolution (HR) TEM (Fig. 1). The nanocrystal was elongated along the *c* axis of anatase, which has a tetragonal structure. The nanocrystal had a truncated rectangular shape, and the lengths of the short *a* axis and the long *c* axis were ~16 and ~34 nm, respectively. According to the previous study,[12] OA and OM adsorb to the {001} and {101} faces of anatase and control the growth rate in the [001] and [101] directions, respectively.

Department of Applied Chemistry, Faculty of Science and Technology, Keio University, 3-14-1, Hiyoshi, Kohoku-ku, Yokohama 223-8522, Japan. E-mail: hiroaki@applc.keio.ac.jp

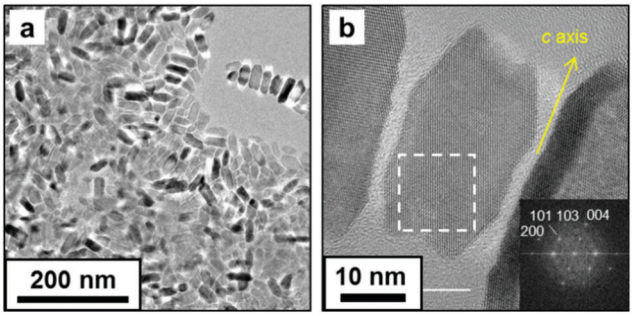

Fig. 1 TEM (a) and HRTEM (b) images of obtained nanocrystals in toluene. The fast Fourier transform (FFT) profile in the dashed square is shown in inset (b).

Moreover, the growth rate of TiO_2 crystals influences the shape of the nanoparticles.[12a] In the present study, the {100} facets of anatase nanocrystals are deduced to be induced by the combined effects of TB, OA, and OM. These anisotropic nanocrystals are appropriate for the assembly of 1D and 2D patterns.

The extraction and redispersion of the resultant nanocrystals in hexane were necessary for separating nanocrystals with similar shapes and sizes. Screened nanocrystals were found to form molecular-mediated alignment, as shown in TEM images (Fig. 2a and b). The ordered 1D alignment occurred in the *a* direction.

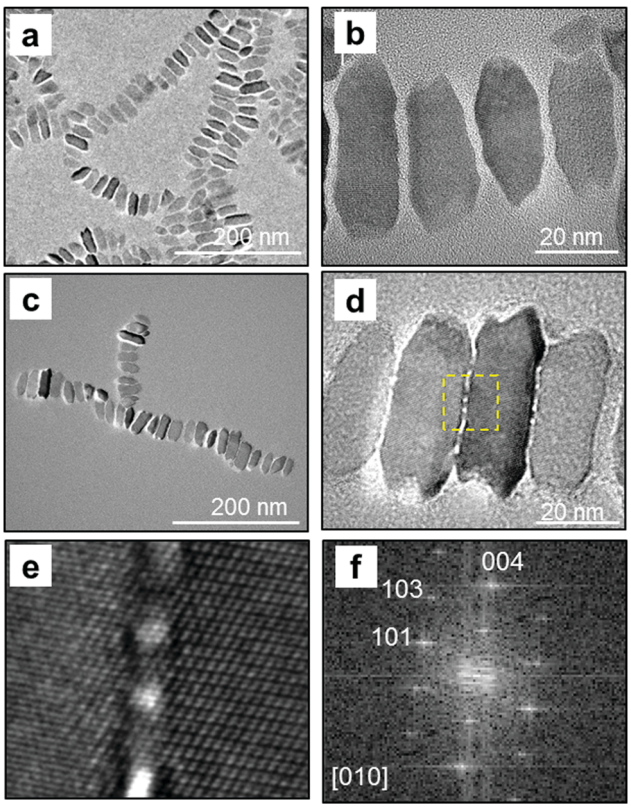

Fig. 2 TEM (a and c) and HRTEM (b, d and e) images of the alignments of TiO_2 nanocrystals on a TEM grid before (a and b) and after (c–e) UV irradiation; the magnified image (e) of the yellow-dashed square in (d) and its FFT profile (f).

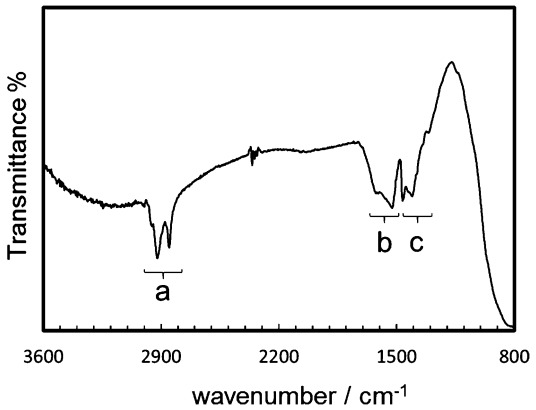

Fig. 3 FTIR spectrum of the obtained TiO_2 powders. The antisymmetric stretching vibration of $-CH_3-$, the antisymmetric and symmetric stretching vibration of $-CH_2-$ groups (a), the scissoring bending vibration of N–H groups, antisymmetric and symmetric stretching vibration of COO^- groups (b), and the bending vibration of C–O–H, $-CH_3-$, and O–H groups (c).

The formation mechanism of the specifically ordered arrays was reported in our previous report.[7c] The nanoblocks are arranged at the liquid–air interface due to their hydrophobic nature. The 1D chains elongated in the ⟨100⟩ direction are formed at the interface through the attachment of the relatively large (100) faces by lateral capillary force when the medium is evaporated. The lengths of interspace between two nanocrystals were 1.7–3.0 nm, which indicated that the organic molecules exist in the interspace. The FTIR spectrum (Fig. 3) indicated the presence of OA and OM on the nanocrystals. The bands in the region (a), 2950, 2920, and 2850 cm^{-1}, are assigned to the antisymmetric stretching vibration of $-CH_3-$ and the antisymmetric and symmetric stretching vibrations of $-CH_2-$ groups, respectively. The bands in the region (b), 1620–1525 cm^{-1}, were assigned to the scissoring bending vibration of groups N–H, and the antisymmetric and symmetric stretching vibrations of COO^- groups. The bands in the region (c), 1460–1405 cm^{-1}, were assigned to the bending vibrations of C–O–H, $-CH_3-$, and O–H groups.[6a,14] The organic molecules mediated the specific alignment of the nanocrystals.

Fig. 2c–f shows TEM images of TiO_2 nanocrystals on a nitrocellulose-coated TEM grid after ~18 h of UV irradiation. The photocatalytic effect decomposed the organic molecules adsorbed on the nanocrystal surface. Continuous lattice fringes through several crystal bridges were observed between the adjacent nanocrystals (Fig. 2e). These results indicate that epitaxial attachment occurred with UV irradiation. The organic molecules on the nanocrystal surface would shrink with decomposition, and two nanocrystals would approach each other. The approximation of nanocrystals with the same *a* direction caused crystallographic fusion without heat. As the organic molecules decomposed, the bare surfaces were crystallographically connected to each other.

In the previous study, 2D clusters with attachment on the *a* faces of Mn_3O_4 nanocuboids were formed with the increasing polarity of the dispersion medium.[7c] Fig. 4a shows the TiO_2 nanoblocks on a TEM grid from their dispersion in tetrahydrofuran (THF), which has a higher polarity than hexane. A number of

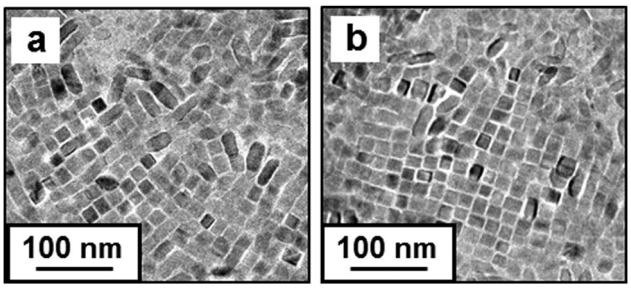

Fig. 4 TEM images of the TiO_2 nanocrystals on TEM grids from the dispersion in tetrahydrofuran (a), and in hexane with additional amounts of OA (b).

square-shaped crystal arrays were observed on the TEM grid. This indicates that 2D arrays with *c* faces parallel to the substrate were obtained in a part of the nanoblocks. In a relatively polar medium, 2D arrays of the hydrophobic nanoblocks are easily formed *via* the attachment of the relatively large (100) faces. The 2D arrays were also obtained from dispersion in hexane in the presence of an additional amount of OA (Fig. 4b). We found the formation of 2D arrays with increasing concentrations of organic molecules. In the previous study, 2D superlattices with the *c* axis vertical to a substrate were obtained with increasing nanocrystals and OA.[13] The excess amount of the surface-mediated molecules enhanced the interaction, such as depletion attraction,[15] between TiO_2 nanocrystals.

Here, crystallographically connected 2D arrays were formed with UV irradiation. The 2D arrays of TiO_2 nanocrystals, in which the *c* face was parallel to the substrate, were obtained on a TEM grid by dispersion in toluene with additional OA and OM. After UV irradiation, the nanocrystals were connected in the arrays (Fig. 5). With UV irradiation, the average distance of interspace was decreased from 2.7 ± 0.50 nm to 0.40 ± 0.51 nm. The decomposition of organic molecules and the epitaxial attachment progressed on four sides of a TiO_2 nanocrystal in the 2D arrays.

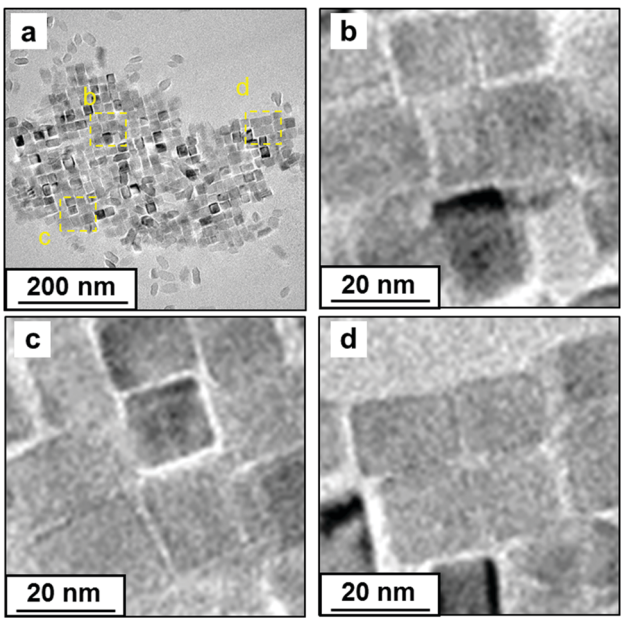

Fig. 5 TEM images of the oriented TiO_2 nanocrystals on a TEM grid after UV irradiation for 14 h (a–d). Images (b–d) show magnified images of the yellow-dashed square in (a).

The 1D alignments of Mn_3O_4 nanoblocks,[7c] that had no photocatalytic activity, were irradiated for 18 h by UV light from the same super high-pressure UV lamp as a reference. The epitaxial attachment with the removal of organic molecules was not observed on the Mn_3O_4 nanoblocks, although UV light would be absorbed by the metal oxide. This suggests that the heat-induced phenomenon is not essential for the epitaxial attachment of TiO_2 nanoblocks under UV irradiation. The organic molecules that were closely attached onto TiO_2 nanoblocks were decomposed by UV irradiation. In this case, the organic molecules would be directly decomposed by the photocatalytic activation rather than the exothermal oxidative reaction with oxygen molecules. Thus, the oxidative pyrolysis is not the key reaction for the epitaxial attachment.

In summary, 1D and 2D alignments of anatase TiO_2 were selectively achieved *via* evaporation-induced assembly. Epitaxial attachment of the nanocrystals in the ordered arrays was induced by the decomposition of organic molecules on nanocrystal surfaces and the approximation of nanocrystals under UV irradiation. Photocatalytic activity enables the crystallographic fusion of oriented nanoblocks through a non-thermal process.

Notes and references

1 (*a*) C. B. Murray, C. R. Kagan and M. G. Bawendi, *Annu. Rev. Mater. Sci.*, 2000, **30**, 545–610; (*b*) K. Zhou and Y. Li, *Angew. Chem., Int. Ed.*, 2012, **51**, 602–613.
2 (*a*) H. Cölfen and M. Antonietti, *Angew. Chem., Int. Ed.*, 2005, **44**, 5576–5591; (*b*) Q. Zhang, S.-J. Liu and S.-H. Yu, *J. Mater. Chem.*, 2009, **19**, 191–207.
3 (*a*) R. L. Penn and J. F. Banfield, *Am. Mineral.*, 1998, **83**, 1077–1082; (*b*) C. Schliehe, B. H. Juarez, M. Pelletier, S. Jander, D. Greshnykh, M. Nagel, A. Meyer, S. Foerster, A. Kornowski, C. Klinke and H. Weller, *Science*, 2010, **329**, 550–553; (*c*) M. Li, H. Schnablegger and S. Mann, *Nature*, 1999, **402**, 393–395; (*d*) C. J. Dalmaschio, C. Ribeiro and E. R. Leite, *Nanoscale*, 2010, **2**, 2336–2345; (*e*) Z. Zhuang, X. Xue and Z. Lin, *Phys. Chem. Chem. Phys.*, 2015, **17**, 4845–4848.
4 (*a*) R. L. Penn and J. F. Banfield, *Geochim. Cosmochim. Acta*, 1999, **63**, 1549–1557; (*b*) M. Adachi, Y. Murata, J. Takao, J. Jiu, M. Sakamoto and F. Wang, *J. Am. Chem. Soc.*, 2004, **126**, 14943–14949; (*c*) C.-S. Tsao, C.-M. Chuang, C.-Y. Chen, Y.-C. Huang, H.-C. Cha, F.-H. Hsu, C.-Y. Chen, Y.-C. Tu and W.-F. Su, *J. Phys. Chem. C*, 2014, **118**, 26332–26340; (*d*) H. Wang, Y. Liu, Z. Liu, H. Xu, Y. Deng and H. Shen, *CrystEngComm*, 2012, **14**, 2278–2282.
5 E. V. Shevchenko, D. V. Talapin, N. A. Kotov, S. O'Brien and C. B. Murray, *Nature*, 2006, **439**, 55–59.
6 (*a*) S. Yang and L. Gao, *J. Am. Chem. Soc.*, 2006, **128**, 9330–9331; (*b*) J. Ren and R. D. Tilley, *J. Am. Chem. Soc.*, 2007, **129**, 3287–3291.
7 (*a*) T. S. Sreeprasad, A. K. Samal and T. Pradeep, *Langmuir*, 2008, **24**, 4589–4599; (*b*) A. Singh, R. D. Gunning, S. Ahmed, C. A. Barrett, N. J. English, J.-A. Garate and K. M. Ryan, *J. Mater. Chem.*, 2012, **22**, 1562–1569; (*c*) Y. Nakagawa, H. Kageyama, Y. Oaki and H. Imai, *J. Am. Chem. Soc.*, 2014, **136**, 3716–3719.
8 Y. Nakagawa, H. Kageyama, Y. Oaki and H. Imai, *Langmuir*, 2015, **31**, 6197–6201.
9 (*a*) G. Liu, H. G. Yang, J. Pan, Y. Q. Yang, G. Q. Lu and H.-M. Cheng, *Chem. Rev.*, 2014, **114**, 9559–9612; (*b*) L. Etgar, W. Zhang, S. Gabriel, S. G. Hickey, M. K. Nazeeruddin, A. Eychmüller, B. Liu and M. Grätzel, *Adv. Mater.*, 2012, **24**, 2202–2206; (*c*) N. Li, G. Zhou, R. Fang, F. Li and H.-M. Cheng, *Nanoscale*, 2013, **5**, 7780–7784.

10 (*a*) R. Menzel, A. Duerrbeck, E. Liberti, H. C. Yau, D. McComb and M. S. P. Shaffer, *Chem. Mater.*, 2013, **25**, 2137–2145; (*b*) T. R. Gordon, M. Cargnello, T. Paik, F. Mangolini, R. T. Weber, P. Fornasiero and C. B. Murray, *J. Am. Chem. Soc.*, 2012, **134**, 6751–6761; (*c*) J. Pan, G. Liu, G. Q. Lu and H.-M. Cheng, *Angew. Chem., Int. Ed.*, 2011, **50**, 2133–2137; (*d*) X. Han, Q. Kuang, M. Jin, Z. Xie and L. Zheng, *J. Am. Chem. Soc.*, 2009, **131**, 3152–3153.

11 (*a*) T.-W. Zeng, Y.-Y. Lin, H.-H. Lo, C.-W. Chen, C.-H. Chen, S.-C. Liou, H.-Y. Huang and W.-F. Su, *Nanotechnology*, 2006, **17**, 5387–5392; (*b*) Y.-Y. Lin, T.-H. Chu, S.-S. Li, C.-H. Chuang, C.-H. Chang, W.-F. Su, C.-P. Chang, M.-W. Chu and C.-W. Chen, *J. Am. Chem. Soc.*, 2009, **131**, 3644–3649; (*c*) Y.-C. Huang, G. C. Welch, G. C. Bazan, M. L. Chabinyc and W.-F. Su, *Chem. Commun.*, 2012, **48**, 7250–7252.

12 (*a*) C.-T. Dinh, T.-D. Nguyen, F. Kleitz and T.-O. Do, *ACS Nano*, 2009, **3**, 3737–3743; (*b*) P. D. Cozzoli, A. Kornowski and H. Weller, *J. Am. Chem. Soc.*, 2003, **125**, 14539–14548; (*c*) B. H. Wu, G. Y. Guo, N. F. Zheng, Z. X. Xie and G. D. Stucky, *J. Am. Chem. Soc.*, 2008, **130**, 17563–17567.

13 Y. Zhang and F.-M. Liu, *RSC Adv.*, 2015, **5**, 66934–66939.

14 M. Kar, R. Agrawal and H. W. Hillhouse, *J. Am. Chem. Soc.*, 2011, **133**, 17239–17247.

15 D. Baranov, A. Fiore, M. V. Huis, C. Giannini, A. Falqui, U. Lafont, H. Zandbergen, M. Zanella, R. Cingolani and L. Manna, *Nano Lett.*, 2010, **10**, 743–749.

